Preprints of the 21st IFAC World Congress (Virtual)
Berlin, Germany, July 12-17, 2020

Towards Insulin Monitoring: Infrequent Kalman Filter Estimates for Diabetes Management ⋆

Kelilah L. Wolkowicz * **Sunil Deshpande** *
Francis J. Doyle III * **Eyal Dassau** *

* *Harvard John A. Paulson School of Engineering and Applied Sciences, Harvard University, MA 02138 USA (e-mail: dassau@ seas.harvard.edu).*

Abstract: We propose a Kalman filter-based observer utilizing noisy remote compartment insulin measurements to estimate plasma insulin concentration. The design considers plant-model mismatch, sensor noise, as well as both uniform sampling intervals, mimicking infrequent continuous measurements, and non-uniform sampling intervals, mimicking infrequent on-demand measurements. The performance of the observer is demonstrated on ten *in-silico* subjects from the UVA/Padova simulator using real-life scenarios, including variability in sensor noise and variability in insulin pharmacokinetics. The proposed observer provides insight into the future use of insulin measurements for diabetes management.

Keywords: Chronic care and/or diabetes, Kalman filters, State estimation, Measurement noise, Sampling intervals, Biomedical system modeling, simulation and visualization

1. INTRODUCTION

Type 1 diabetes (T1D) is a disease that prevents the body from properly producing insulin and requires tracking and control of blood glucose (BG) levels. For effective BG management, both those with diabetes and their families must learn to calculate the correct insulin dosage, as well as understand the effect of insulin dosage with regards to varying meal contents, physical activity, illness, and stress, in addition to other aspects related to their treatment. While there have been significant improvements in measurement techniques for BG monitoring, limited research has focused on advancing insulin measurement devices. Conventional methods of BG monitoring now require only a small amount of blood acquired through either finger pricking, called self-monitoring blood glucose (SMBG), or a thin sensor inserted subcutaneously, providing continuous monitoring and aptly called continuous glucose monitoring (CGM) (Villena Gonzales et al., 2019). Insulin sensors would provide additional information that could be used as feedback for insulin infusion systems, insulin pumps, and even for enhanced control of automatic insulin delivery systems, such as an artificial pancreas (AP).

Currently, insulin measurements can be obtained within a laboratory using whole blood, serum, or plasma measurements via immunoassays that cannot be used in ambulatory settings (Vargas et al., 2019). However, recent technological advances in insulin sensor capability may soon allow for on-demand insulin information, similar to SMBG meters (Wang and Zhang, 2001; Bisker et al., 2015; Vargas et al., 2019; Kartal et al., 2019). These sensors have the potential to lead to point-of-care (POC) measurements, advancing personalized diabetes management with estimates of insulin (Wang and Zhang, 2001; Vargas et al., 2019).

This advancement may lead to exciting new opportunities for glycemic control, but first, one must consider sensor limitations, as well as *how* this new insulin information can be used. Similar to SMBG meters, errors can arise from insulin measurements, including both sensor system errors and user errors (Staal et al., 2018). Even with the technological advances in sensor design, all sensors are still prone to inherent and systemic noise, as well as biofouling, bias, and latencies. These challenges must be balanced with models that are robust to erroneous insulin measurements if they are to be used to further improve diabetes management.

While continuous real-time sampling is the paramount objective, initial insulin sensors are primed for infrequent on-demand measurements. On-demand insulin measurements will allow the user to monitor their insulin at discrete times throughout the day, as a corollary to SMBG, most likely two to three times per day (Gonder-Frederick et al., 1988), though recommended four or more times per day (Rewers et al., 2014). Looking forward to insulin sensor commercialization, how frequently measurements should be obtained is an important consideration. While every half hour or even every hour may not yet be feasible, measurements every two to three hours may still provide the user with usable insulin updates, in addition to being used for closed-loop control.

A current limitation of AP systems is the estimation of active insulin concentrations. Knowing insulin information may allow for faster automated insulin system re-

⋆ This work was made possible with support from The Leona M. and Harry B. Helmsley Charitable Trust (Grant no. 2018PG-TID061).

sponses; the pending effect of insulin on glucose may be detected earlier under different physiological conditions, such as changing insulin sensitivity. Many AP designs do not integrate insulin measurements, but instead approximate insulin-on-board (IOB) to correct for any remaining insulin from the last injection or infusion (Rodriguez-Saldana, 2019; Gondhalekar et al., 2018). Since insulin cannot yet be measured in real-time, measurements of interstitial glucose concentration via glucose-insulin models are used to estimate insulin concentration (Hajizadeh et al., 2019, 2017; de Pereda et al., 2016; Haidar et al., 2013; Dalla Man et al., 2007; Hovorka et al., 2004). For example, de Pereda et al. (2016) and Hajizadeh et al. (2017, 2019) demonstrate the performance of their respective Extended Kalman Filter algorithms in simulation. To account for the high intra- and inter-subject variability in insulin pharmacokinetic (PK) dynamics, both utilized personalized insulin PK models. While each approach demonstrates plasma insulin concentration estimation, neither uses insulin-based measurements.

This paper proposes a Kalman Filter (KF) that utilizes noisy remote compartment insulin measurements to estimate plasma insulin concentration. The KF design is evaluated by its utility for three primary challenges: plant-model mismatch, insulin PK variability, and infrequent sensor measurements for both uniform and nonuniform measurement intervals. The performance of the observer is demonstrated on ten *in-silico* subjects from the United States Food and Drug Administration-accepted University of Virginia (UVA)/Padova T1D Metabolic Simulator (Dalla Man et al., 2014) using real-life use-case scenarios, including variability in sensor noise and insulin PK. The ability to monitor and integrate insulin information will allow users to make more informed decisions regarding insulin dosing, thus helping to prevent hypoglycemia and improving diabetes management.

The remainder of this paper is organized as follows: The insulin PK model is introduced in Section 2. In Section 3, the KF insulin observer is developed. For completeness, details of the process and measurement noise covariance tuning, as well as sample time requirements are addressed. The *in-silico* implementation of the KF within the UVA/Padova T1D Metabolic Simulator is discussed in Section 4. Conclusions and future work are presented in Section 5.

2. INSULIN PHARMACOKINETIC MODELS

The patient-specific insulin PK model proposed in Schiavon et al. (2017), which models the subcutaneous (SC) absorption of fast-acting insulin, was used as a basis for the presented model. First, the model includes a subject-specific delay τ (min) in the appearance of insulin by injection $\mathbf{u}$ (pmol/kg per min). The insulin injection appears in the first SC compartment I_{SC1} (pmol/kg), which represents insulin in a non-monomeric state. From the first compartment, insulin is partially absorbed into plasma I_P (pmol/kg) with a nonmonomeric insulin absorption rate constant k_{a1} (min^{-1}), while the remaining insulin diffuses with a nonmonomeric insulin dissociation rate constant k_d (min^{-1}) into a second compartment I_{SC2} (pmol/kg), representing insulin in the monomeric state. Then, insulin is finally absorbed into plasma with a

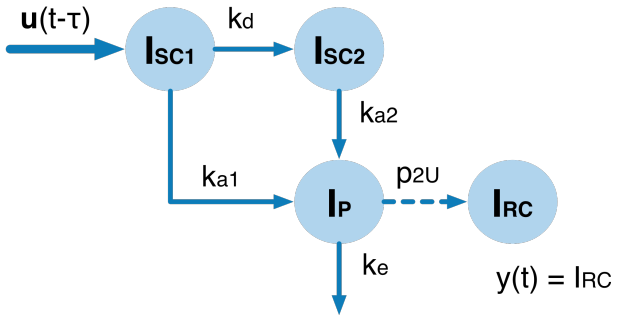

Fig. 1. Model of insulin PK with inputs of administered insulin and measurements of I_{RC}. Figure adapted from Schiavon et al. (2017).

monomeric insulin absorption rate constant k_{a2} (min^{-1}). Model parameters of plasma insulin kinetics are the volume of insulin distribution V_i (L/kg) and the fractional clearance rate k_e (min^{-1}). The person-specific parameters are reported in Kovatchev et al. (2010) and Schiavon et al. (2017). The conversion factor used between conventional and SI units for human insulin is 1 IU = 6000 pmol.

Using this model, the insulin concentration in the SC and plasma compartments are defined as:

$$\dot{I}_{SC1} = -(k_{a1} + k_d)I_{SC1} + \mathbf{u}(t-\tau) \quad (1)$$

$$\dot{I}_{SC2} = -k_{a2}I_{SC2} + k_d I_{SC1} \quad (2)$$

$$\dot{I}_P = -k_e I_P + k_{a1}I_{SC1} + k_{a2}I_{SC2} \quad (3)$$

In an effort to further examine insulin diffusion concentrations, the model was expanded to include insulin in a remote compartment I_{RC}, which represents the delayed appearance of insulin from the plasma compartment and acts as the measured state ($\mathbf{y}(t) = I_{RC}$). The model for the I_{RC} compartment is reported in Dalla Man et al. (2007):

$$\dot{I}_{RC} = -p_{2U}I_{RC} + p_{2U}(\frac{I_P}{Vi} - I_b) \quad (4)$$

where p_{2U} is the rate constant of insulin action on the peripheral glucose utilization and I_b is basal plasma insulin. A pictorial rendition of the insulin PK model is presented in Fig. 1. Since the Simulator contains certain features that are not present within the PK model, specifically, hepatic insulin, inherent plant-model mismatch is present within the model. It is important to note that this PK model is a preliminary proof-of-concept and may require further refinement; clinical experimentation is needed before the model can be validated.

3. INSULIN OBSERVER DESIGN AND TUNING

The aim of this section is to describe the design of the KF insulin observer. The section begins with the derivation of the KF insulin observer to estimate I_P from noisy I_{RC} measurements. Considerations for covariance tuning and sampling time are then discussed.

3.1 Kalman Filter Design

With a model in place to approximate the insulin PK, an observer to estimate the various insulin states was developed. A KF was chosen as the observer because it supports

a real-time model for making estimates of the current insulin state and is equipped to handle state estimates for measurements sampled at various frequencies.

A KF insulin observer was developed by augmenting Eqns. (1)-(3) with Eqn. (4). The subsequent addition of I_b as a state for parameter estimation results in the following continuous-time model:

$$\begin{bmatrix} \dot{I}_{SC1} \\ \dot{I}_{SC2} \\ \dot{I}_P \\ \dot{I}_{RC} \\ \dot{I}_b \end{bmatrix} = \begin{bmatrix} -(k_{a1}+k_d)I_{SC1} + u(t-\tau) \\ k_d I_{SC1} - k_{a2} I_{SC2} \\ k_{a1} I_{SC1} + k_{a2} I_{SC2} - k_e I_P \\ -p_{2U} I_{RC} + p_{2U}(\frac{I_P}{Vi} - I_b) \\ 0 \end{bmatrix} \tag{5}$$

Because patient-specific information is not available for the input delay τ, the median value of 7.6 minutes was used for all *in-silico* subject scenarios (Schiavon et al., 2017).

Discretizing Eqn. (5) via forward Euler integration, we obtain the associated discrete-time state-space equations:

$$\mathbf{x}_{k+1} = \mathbf{A}_d \mathbf{x}_k + \mathbf{B}_d \mathbf{u}_{k-\Delta t\tau} + \mathbf{w}_k \tag{6}$$

$$\mathbf{y}_k = \mathbf{C}_d \mathbf{x}_k + \mathbf{D}_d \mathbf{u}_{k-\Delta t\tau} + \mathbf{v}_k \tag{7}$$

where $\mathbf{x}$ is the state vector of the insulin concentration in each compartment, $\mathbf{A}_d$ is the discrete-time PK model matrix, $\mathbf{B}_d$ is the discrete-time input matrix for the control input of SC insulin administration $\mathbf{u}$, and $\mathbf{C}_d$ is the discrete-time measurement matrix of the measured state $\mathbf{y}$, in this case I_{RC} concentration. Covariances $\mathbf{v}$ and $\mathbf{w}$ are discrete zero-mean white noise sources:

$$\mathbf{w}_k \sim N(0, \mathbf{Q}) \tag{8}$$

$$\mathbf{v}_k \sim N(0, \mathbf{R}) \tag{9}$$

where $\mathbf{Q}$ is the process noise covariance acting on I_{SC1}, and $\mathbf{R}$ is the measurement noise covariance acting on I_{RC}. The expanded form of the discrete-time state-space model is presented in Eqns. (10) and (11), where Δt is a fixed time step of five minutes, comparable to the insulin administration input rate, as well as the standard time interval of CGM measurements, were the observer to integrate glucose states in future research. The time step should not be confused with the measurement sampling intervals T_s, which will be discussed in more detail throughout the remainder of the paper.

3.2 Kalman Filter Prediction and Correction

Once the discretized model has been defined, the KF prediction step can be carried out using the standard KF equations (Simon, 2006):

$$\hat{\mathbf{x}}_{k+1|k} = \mathbf{A}_d \hat{\mathbf{x}}_{k|k} + \mathbf{B}_d \mathbf{u}_{k-\Delta t\tau} + 0 \tag{12}$$

$$\mathbf{P}_{k+1|k} = \mathbf{A}_d \mathbf{P}_{k|k} \mathbf{A}_d^T + \mathbf{Q} \tag{13}$$

where $\hat{\mathbf{x}}_{k|k}$ represents the propagated state at the current time step, $\hat{\mathbf{x}}_{k+1|k}$ is the propagated and updated state from the previous time step, and $\mathbf{u}_k$ is the most recent insulin injection. The third term in the estimated state equation, Eqn. (6), conveys the assumed zero noise associated with the input. The state covariance matrix $\mathbf{P}$ is propagated using the PK model matrix and $\mathbf{Q}$.

The measurement, or correction, step for the state estimate and covariance is then performed using the standard KF equations:

$$\mathbf{K}_{k+1} = \mathbf{P}_{k+1|k} \mathbf{C}_d^T [\mathbf{C}_d \mathbf{P}_{k+1|k} \mathbf{C}_d^T + \mathbf{R}]^{-1} \tag{14}$$

$$\hat{\mathbf{x}}_{k+1|k+1} = \hat{\mathbf{x}}_{k+1|k} + \mathbf{K}_{k+1} [\mathbf{y}_{k+1} - \mathbf{C}_d \hat{\mathbf{x}}_{k+1|k}] \tag{15}$$

$$\mathbf{P}_{k+1|k+1} = [\mathbf{I} - \mathbf{K}_{k+1} \mathbf{C}_d] \mathbf{P}_{k+1|k} \tag{16}$$

where $\mathbf{K}$ is the optimal KF gain, which minimizes the residual error. While KF updates are only performed at prescribed measurement sample intervals T_s to compare the accuracy of the estimates to the actual I_{RC} concentration values, KF predictions are performed for each time step Δt, i.e., every five minutes.

3.3 Process and Measurement Noise Covariance Tuning

A key challenge when designing a KF is correctly characterizing the uncertainties in both the measurements and state dynamics. An incorrect choice of noise characteristics can lead to deterioration in the performance of the state estimator, and potentially result in the estimator diverging from the model and measurements (Bavdekar et al., 2011). Typically, it can be assumed that measurement noise covariance $\mathbf{R}$ is known or can be obtained from measurement data. As the noise level of the insulin sensors is yet to be determined, we investigate the effect of noise on the KF design and measurement sampling intervals by varying added sensor noise, while fixing the tuning for both $\mathbf{Q}$ and $\mathbf{R}$ (Eqns. (17) and (18)) across all subjects and scenarios. The KF measurement noise covariance $\mathbf{R}$ standard deviation was defined as 6.0 pmol/L in order to observe how unknown noise estimates also affect the performance of the observer (Vargas et al., 2019). Additionally, to reproduce real-life scenarios in which PK models may deviate from actual insulin dynamics, measurements were given more tractable weighting, while still maintaining a balance with the insulin PK model.

$$\mathbf{Q} = \begin{bmatrix} 20^2 & 0 & \cdots & 0 \\ 0 & 0 & \cdots & 0 \\ \vdots & \vdots & \ddots & \vdots \\ 0 & 0 & \cdots & 0 \end{bmatrix}_{5\times 5} \tag{17}$$

$$\mathbf{R} = 6^2 \tag{18}$$

3.4 Sample Time Requirements

To create more realistic applications of the insulin observer, both infrequent uniform and nonuniform sampling intervals T_s were addressed. After a SC injection, insulin levels peak after approximately 90 minutes and then slowly dissipates in four to six hours (Jansson et al., 1993; Rajamand et al., 2005). Thus, we invest two use-cases to monitor insulin during elevated concentrations. First, uniform sampling at prescribed measurement intervals were used to mimic infrequent continuous measurements, similar to CGM, at measurement intervals (T_s) of 5, 30, 60, 120, and 180 minutes. Considering the older BG meter models, the first insulin sensors will most likely be used for on-demand insulin measurement at the user's discretion. Subsequently, non-uniform sampling intervals were used to mimic SMBG meters, in which infrequent on-demand measurements are taken throughout the day.

$$\underbrace{\begin{bmatrix} I_{SC1} \\ I_{SC2} \\ I_P \\ I_{RC} \\ I_b \end{bmatrix}}_{\mathbf{x}_{k+1}} = \underbrace{\begin{bmatrix} 1-\Delta t(k_{a1}+k_d) & 0 & 0 & 0 & 0 \\ \Delta t k_d & 1-\Delta t k_{a2} & 0 & 0 & 0 \\ \Delta t k_{a1} & \Delta t k_{a2} & 1-\Delta t k_e & 0 & 0 \\ 0 & 0 & \frac{\Delta t p_{2U}}{Vi} & 1-\Delta t p_{2U} & -\Delta t p_{2U} \\ 0 & 0 & 0 & 0 & 1 \end{bmatrix}}_{\mathbf{A}_d} \underbrace{\begin{bmatrix} I_{SC1} \\ I_{SC2} \\ I_P \\ I_{RC} \\ I_b \end{bmatrix}}_{\mathbf{x}_k} + \underbrace{\begin{bmatrix} \Delta t \\ 0 \\ 0 \\ 0 \\ 0 \end{bmatrix}}_{\mathbf{B}_d} \mathbf{u}_{k-\Delta t\tau} + \mathbf{w}_k \tag{10}$$

$$\underbrace{[I_{RC}]}_{\mathbf{y}_k} = \underbrace{[0\ 0\ 0\ 1\ 0]}_{\mathbf{C}_d} \underbrace{\begin{bmatrix} I_{SC1} \\ I_{SC2} \\ I_P \\ I_{RC} \\ I_b \end{bmatrix}}_{\mathbf{x}_k} + \underbrace{[0]}_{\mathbf{D}_d} \mathbf{u}_{k-\Delta t\tau} + \mathbf{v}_k \tag{11}$$

4. INSULIN OBSERVER IMPLEMENTATION

The KF was evaluated by its utility for three primary challenges: 1) model approximation; 2) variability in insulin PK; and 3) infrequent sensor measurements. In the first challenge, plant-model mismatch and sensor noise were addressed within the context of the observer. Second, variations in subject PK, such as an individual's net insulin elimination and utilization were analyzed to observe the performance of the KF. The third challenge considers non-uniform sampling intervals.

The performance of the observer was demonstrated on ten *in-silico* subjects from the UVA/Padova T1D Metabolic Simulator (Dalla Man et al., 2014) using the three real-life scenario challenges. Every scenario was tested on the ten *in-silico* subjects for multiple repetitions, in which a single random noise generator was used per patient to ensure independence across subjects, as well as reproducibility. The protocol consisted of an eight-hour simulation with one 75-g carbohydrate meal and a person-specific bolus based on their carb-ratio given 65 minutes into the simulation. The simulation scenario was chosen to observe the performance of the KF during both fasting and postprandial states. The KF was initialized with known individualized values (i.e., $\mathbf{x}_0 = [I_{SC1,0}\ I_{SC2,0}\ I_b V_i\ 0\ I_b]$) that were sensitive to noise in order to also observe the convergence of the KF with incorrect initial states. The performance of the insulin observer estimates was evaluated by computing root-mean-square error (RMSE) to determine the standard deviation of the residuals, or prediction errors, from the I_P concentration obtained from the UVA/Padova Simulator.

4.1 Nominal Performance of Insulin Observer Under Variations in Sample Time and Noise

The first challenge considers plant-model mismatch, comparing a person-specific individualized model across uniform sampling times and noise standard deviations. Twenty-five cases, with 50 repetitions per subject, were run in order to evaluate measurement samples of 5-, 30-, 60-, 120-, and 180-minute intervals, as well as the open-loop case with no measurements, across noise standard deviations of 1, 3, 6, 9, 12, 16, and 20 pmol/L.

The median RMSE values are shown in Fig. 2 and demonstrate the expected improved performance of the insulin observer with more frequent uniform sampling intervals and reduced sensor noise. From the RMSE values, it was

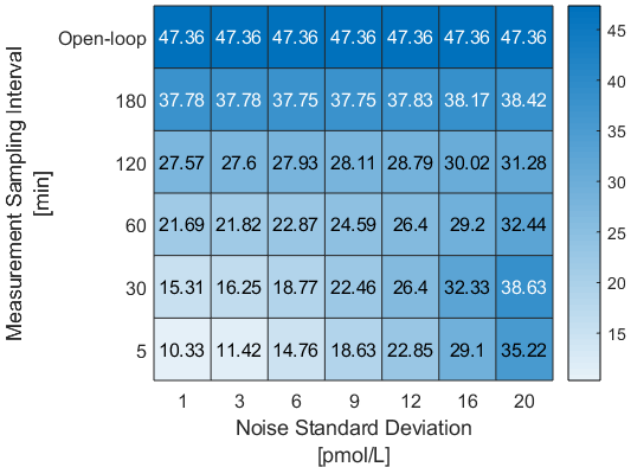

Fig. 2. *In-silico* KF median RMSE (pmol/L) as a function of measurement sampling time and sensor noise. All sampling times begin at the start of the simulation.

also observed that the insulin observer's sensitivity to noise decreased as measurement intervals increased (i.e., as measurement frequency decreases from 5- to 180-minute intervals). Noise sensitivity was calculated as

$$S = \frac{RMSE_{N(0,1)} - RMSE_{N(0,20)}}{RMSE_{N(0,1)}} \times 100\%, \tag{19}$$

where $RMSE_{N(0,1)}$ and $RMSE_{N(0,20)}$ are the RMSE values of measurement sampling interval T_s for noise standard deviations of 1 and 20 pmol/L, respectively. The individualized model's noise sensitivity falls from 241.05%, 152.31%, 49.59%, 13.43%, to 1.71% for measurement intervals of 5, 30, 60, 120, and 180 minutes, respectively. This result seems to infer that, as noise increases, there is a greater cost for more frequent sampling due to sensitivity to noise. However, if the true sensor noise level was known, R could be more finely tuned for improved performance. The open-loop RMSE value was found to be 47.36 pmol/L, which reasonably indicates no measurements result in degraded performance of the KF.

4.2 Variability in Insulin Pharmacokinetics

The second challenge considers enforced changes in insulin PK variability. Within the UVA/Padova, fifty repetitions per subject were run and three parameters, m_1, m_2, and m_4 were modified in the insulin subsystem:

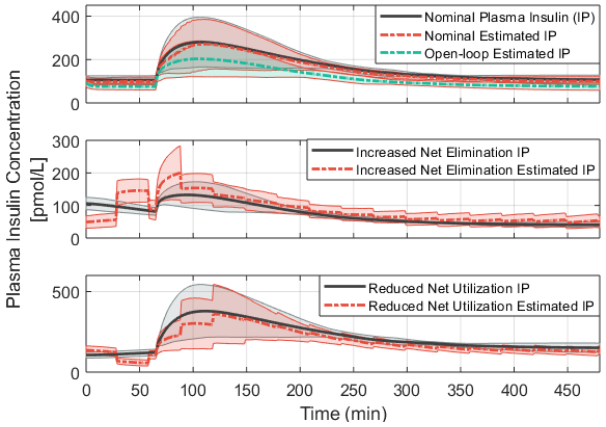

Fig. 3. Median and IQR ranges for enforced PK modifications utilizing 30-minute measurement intervals at a noise standard deviation of 6 pmol/L; I_P represented by solid lines and $\hat{I}_P$ by dotted lines. **Top:** Nomimal (i.e. non-modified) and open-loop. **Middle:** Increased net elimination. **Bottom:** Reduced net utilization.

$$\dot{I}_P = -(m_2 + m_4)I_P + m_1 I_L + k_{a1} I_{SC1} + k_{a2} I_{SC2} \quad (20)$$

where I_L is hepatic insulin concentration; m_1, m_2, and m_4 are the insulin kinetic rate parameters (Kovatchev et al., 2010; Dalla Man et al., 2014). Two insulin PK modifications were made: 1) increased net elimination via decreasing m_1 by 25% and increasing $(m_2 + m_4)$ by 150%; and 2) reduced net utilization via increasing m_1 by 25% and decreasing $(m_2 + m_4)$ by 25%. Insulin elimination occurs when the liver and kidneys metabolize insulin so that it is no longer functional, while insulin utilization occurs when cells and tissues use insulin to absorb glucose. The asymmetric kinetic rate parameter modifications were chosen to obtain more symmetric results in terms of fasting plasma insulin rates (e.g., reduce/increase equilibrium by ± 50 pmol/L). By changing these parameters within the simulator, we are able to observe how the KF performs when metabolic parameters are incorrectly defined. Additionally, it provides an opportunity to see how the KF performs in terms of estimating insulin peak dynamics. Five cases were run to evaluate time samples of 5-, 30-, 60-, 120-, and 180-minute intervals for a noise standard deviation of 6.0 pmol/L.

The purpose of this real-life scenario was to observe not only the performance of the insulin estimator with unknown or changing PK dynamics, but also the change in insulin action peak time during these cases. In Fig. 3, it is observed that increased net elimination (middle) results in faster peak times, with a median peak time at 93 minutes into the simulation (28 minutes after the meal), while reduced net utilization (bottom) results in slower peak times, with a median peak time at 111 minutes (46 minutes post meal); the median nominal peak time occurred at 100 minutes (35 minutes post meal). The results demonstrate a clear trend in relative peak times in regards to increased insulin elimination, with faster peak times at lower concentrations, versus reduced utilization, with slower peak times at higher concentrations. From these dynamics, it is also observed that the KF filter overestimates increased net elimination and underestimates reduced net utilization.

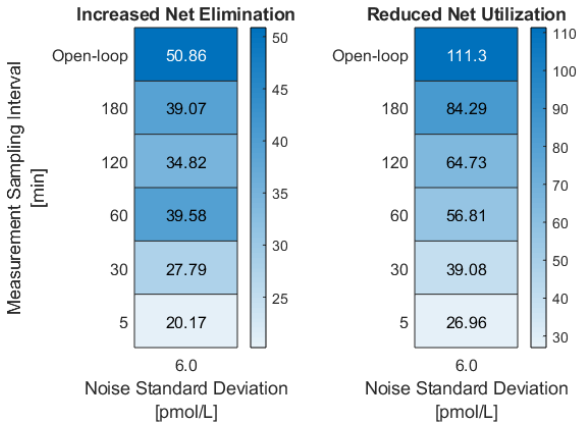

Fig. 4. *In-silico* KF median RMSE (pmol/L) as a function of measurement sampling time, including no measurements in open-loop, for enforced PK variations.

Underestimating insulin concentrations is far more dangerous when attempting to estimate someone's current insulin concentration – a user may think they have less insulin on board then is the case. As such, insulin measurements to update the model become much more important.

The median RMSE values are reported in Fig. 4, where again a clear trend in increasing median and interquartile (IQR) RMSE of 20.17 (6.84) to 39.07 (13.04) pmol/L and of 26.96 (8.40) to 84.29 (29.54) pmol/L is observed for increasing measurement sampling intervals from 5 to 180 minutes for increased net elimination and reduced net utilization, respectively. Increased net elimination yields improved KF performance compared to reduced net utilization. This result may be due to the tighter concentration range for increased elimination (note the change in the y-axis in Fig. 3); more constrained measurement variations allow for improved KF performance than measurements taken with a higher variance. Additionally, while the nominal open-loop performance yielded an RMSE of 47.36 pmol/L, the two modified PK scenarios yielded open-loop RMSE of 50.86 pmol/L and 111.3 pmol/L, respectively.

4.3 Infrequent On-Demand Measurements

In an effort to simulate a realistic scenario using a potential typical user's relaxed use of the recommended SMBG measurement times (Rewers et al., 2014), the third challenge utilizes insulin measurements provided only three times over the eight-hour simulation period with a noise standard deviation of 6.0 pmol/L. The on-demand measurement times were randomly initiated, but set in time bands, indicated in Fig. 5, to reproduce when a user may likely take an insulin measurement: 1) prior to the meal, within the first 65 minutes of the simulation; 2) within the next two to three hours after the meal, from 66 to 240 minutes; and 3) at any point after the second measurement, but still within the eight-hour period, from 241 to 480 minutes (e.g. this measurement may have been during the night, for instance, if the meal provided is dinner). The measurements were randomly generated to occur within their banded periods and this challenge included 400 repetitions per subject.

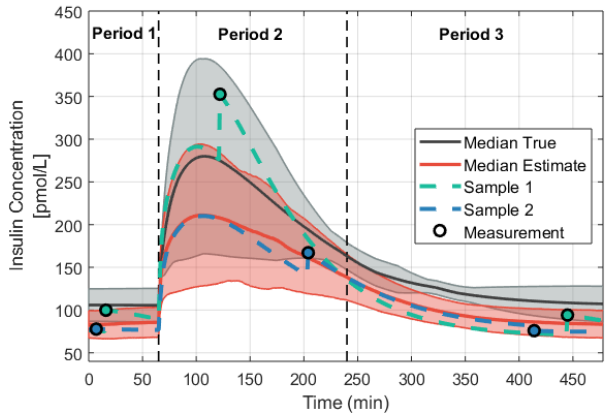

Fig. 5. Median and IQR ranges for nonuniform sampling with a noise standard deviation of 6 pmol/L. I_P concentration is presented in grey; $\hat{I}_P$ concentration is presented in red; $\hat{I}_P$ for two sample cases are represented by dashed lines with measurements indicated by a black '**O**'.

Figure 5 presents the median and IQR ranges of the actual and estimated I_P concentration, as well as two sample cases for the on-demand measurement challenge. It was observed that the time at which the measurements occur are crucial to detecting changes in insulin PK dynamics, particularly insulin peak times. For example, a measurement taken shortly after the meal in Sample 1 provides the observer with more information to better predict the insulin peak. In Sample 2, however, the second measurement was taken almost two and a half hours after the meal, and the interesting dynamics of the insulin peak were likely underestimated.

The median (IQR) RMSE value was 38.47 (10.16) pmol/L, yielding an 18.77% improvement in KF performance compared to no measurements in open-loop (see Fig. 2). Uniform and nonuniform performance cannot be equitably compared due to the measurement sampling procedure for each scenario. For the uniform scenarios, all measurements were initialized to begin at the start of the simulation ($t = 0$), and each was then uniformly sampled at the prescribed measurement interval, meaning all 5-minute measurement samples occurred at exactly the same points in time, and equivalently for measurement intervals of 30 to 180 minutes. Consequently, some of the more challenging insulin dynamics were missed, particularly as the intervals between measurements increased. Additionally, up until the first measurement, the KF relied solely on the model for the prediction, and no noise was contributed to the scenario before that first measurement. Moreover, noise was only contributed during the defined measurement time. Conversely, for the nonuniform scenario, the three measurements could be taken at any point within the eight-hour period, and thus, noise was continuously contributed to the model estimates when determining RMSE for the 4000 individual nonuniform cases.

5. CONCLUSIONS

The proposed observer provides insight into the future use of insulin monitoring for diabetes management. Overall, more frequent uniform sampling and reduced sensor noise resulted in improved performance of the insulin observer. However, as noise increased, there appeared to be a greater cost for more frequent sampling due to noise sensitivity. This result may infer that that less frequent sampling is needed, when in reality, the true sensor noise level is still unknown, and thus Q and R may need finer tuning. Moreover, as the PK model is refined and verified, the KF performance will further improve. Variability in insulin PK was also detected when examining trends in insulin peak times. Finally, it was found that the observer produced reliable estimates even for very infrequent on-demand insulin measurements.

The presented uniform sampling scenarios were initialized to began at the start of the simulation, and then only procured a measurement at the prescribed sample interval. Future work will integrate randomized sampling times within the uniform sampling intervals to better compare the uniform and nonuniform scenarios. Additionally, future extensions will evaluate the inclusion of capillary insulin within the PK model, which may ultimately provide improved approximations of estimated insulin concentrations.

While no current recommendations exist as to how often insulin measurements should occur, the proposed insulin observer demonstrates that even three measurements within an eight-hour period provide useful insulin information. Ultimately, monitoring insulin information and integrating estimated concentrations within feedback systems will allow those with diabetes to make more informed decisions regarding insulin dosing, helping to prevent hypoglycemic events and improving diabetes management.

ACKNOWLEDGEMENTS

Access to the academic version of the UVA/Padova Metabolic Simulator was provided by an agreement with Prof. C. Cobelli (University of Padova) and Prof. B. P. Kovatchev (UVA) for research purposes.

REFERENCES

Bavdekar, V.A., Deshpande, A.P., and Patwardhan, S.C. (2011). Identification of process and measurement noise covariance for state and parameter estimation using extended kalman filter. *Journal of Process Control*, 21(4), 585–601.

Bisker, G., Iverson, N.M., Ahn, J., and Strano, M.S. (2015). A pharmacokinetic model of a tissue implantable insulin sensor. *Advanced Healthcare Materials*, 4(1), 87–97.

Dalla Man, C., Micheletto, F., Lv, D., Breton, M., Kovatchev, B., and Cobelli, C. (2014). The uva/padova type 1 diabetes simulator: new features. *Journal of Diabetes Science and Technology*, 8(1), 26–34.

Dalla Man, C., Rizza, R.A., and Cobelli, C. (2007). Meal simulation model of the glucose-insulin system. *IEEE Transactions on Biomedical Engineering*, 54(10), 1740–1749.

de Pereda, D., Romero-Vivo, S., Ricarte, B., Rossetti, P., Ampudia-Blasco, F.J., and Bondia, J. (2016). Real-time estimation of plasma insulin concentration from continuous glucose monitor measurements. *Computer*

Methods in Biomechanics and Biomedical Engineering, 19(9), 934–942.

Gonder-Frederick, L.A., Julian, D.M., Cox, D.J., Clarke, W.L., and Carter, W.R. (1988). Self-measurement of blood glucose: accuracy of self-reported data and adherence to recommended regimen. *Diabetes Care*, 11(7), 579–585.

Gondhalekar, R., Dassau, E., and Doyle III, F.J. (2018). Velocity-weighting & velocity-penalty mpc of an artificial pancreas: Improved safety & performance. *Automatica*, 91, 105–117.

Haidar, A., Elleri, D., Kumareswaran, K., Leelarathna, L., Allen, J.M., Caldwell, K., Murphy, H.R., Wilinska, M.E., Acerini, C.L., Evans, M.L., et al. (2013). Pharmacokinetics of insulin aspart in pump-treated subjects with type 1 diabetes: reproducibility and effect of age, weight, and duration of diabetes. *Diabetes Care*, 36(10), e173–e174.

Hajizadeh, I., Rashid, M., and Cinar, A. (2019). Plasma-insulin-cognizant adaptive model predictive control for artificial pancreas systems. *Journal of Process Control*, 77, 97–113.

Hajizadeh, I., Turksoy, K., Cengiz, E., and Cinar, A. (2017). Real-time estimation of plasma insulin concentration using continuous subcutaneous glucose measurements in people with type 1 diabetes. In *2017 American Control Conference (ACC)*, 5193–5198. IEEE.

Hovorka, R., Canonico, V., Chassin, L.J., Haueter, U., Massi-Benedetti, M., Federici, M.O., Pieber, T.R., Schaller, H.C., Schaupp, L., Vering, T., et al. (2004). Nonlinear model predictive control of glucose concentration in subjects with type 1 diabetes. *Physiological Measurement*, 25(4), 905.

Jansson, P.A.E., Fowelin, J.P., Von Schenck, H.P., Smith, U.P., and Lönnroth, P.N. (1993). Measurement by microdialysis of the insulin concentration in subcutaneous interstitial fluid: importance of the endothelial barrier for insulin. *Diabetes*, 42(10), 1469–1473.

Kartal, F., Çimen, D., Bereli, N., and Denizli, A. (2019). Molecularly imprinted polymer based quartz crystal microbalance sensor for the clinical detection of insulin. *Materials Science and Engineering: C*, 97, 730–737.

Kovatchev, B.P., Gonder-Frederick, L., Cox, D.J., and Clarke, W.L. (2010). Method, system and computer program product for evaluating the accuracy of blood glucose monitoring sensors/devices. US Patent 7,815,569.

Rajamand, N., Ungerstedt, U., and Brismar, K. (2005). Subcutaneous microdialysis before and after an oral glucose tolerance test: a method to determine insulin resistance in the subcutaneous adipose tissue in diabetes mellitus. *Diabetes, Obesity and Metabolism*, 7(5), 525–535.

Rewers, M.J., Pillay, K., De Beaufort, C., Craig, M.E., Hanas, R., Acerini, C.L., and Maahs, D.M. (2014). Assessment and monitoring of glycemic control in children and adolescents with diabetes. *Pediatric Diabetes*, 15(S20), 102–114.

Rodriguez-Saldana, J. (2019). *The Diabetes Textbook: Clinical Principles, Patient Management and Public Health Issues*. Springer.

Schiavon, M., Dalla Man, C., and Cobelli, C. (2017). Modeling subcutaneous absorption of fast-acting insulin in type 1 diabetes. *IEEE Transactions on Biomedical Engineering*, 65(9), 2079–2086.

Simon, D. (2006). *Optimal state estimation: Kalman, H infinity, and nonlinear approaches*. John Wiley & Sons.

Staal, O.M., Sælid, S., Fougner, A., and Stavdahl, Ø. (2018). Kalman smoothing for objective and automatic preprocessing of glucose data. *IEEE Journal of Biomedical and Health Informatics*, 23(1), 218–226.

Vargas, E., Teymourian, H., Tehrani, F., Eksin, E., Sánchez-Tirado, E., Warren, P., Erdem, A., Dassau, E., and Wang, J. (2019). Enzymatic/immunoassay dual-biomarker sensing chip: Towards decentralized insulin/glucose detection. *Angewandte Chemie International Edition*, 58(19), 6376–6379.

Villena Gonzales, W., Mobashsher, A.T., and Abbosh, A. (2019). The progress of glucose monitoring—a review of invasive to minimally and non-invasive techniques, devices and sensors. *Sensors*, 19(4), 800.

Wang, J. and Zhang, X. (2001). Needle-type dual microsensor for the simultaneous monitoring of glucose and insulin. *Analytical Chemistry*, 73(4), 844–847.